RESEARCH ARTICLE

Soluble bone-derived osteopontin promotes migration and stem-like behavior of breast cancer cells

Graciella M. Pio[1], Ying Xia[2], Matthew M. Piaseczny[1], Jenny E. Chu[1], Alison L. Allan[1,2,3,4]*

1 Department of Anatomy & Cell Biology, Schulich School of Medicine & Dentistry, University of Western University, London, ON, Canada, **2** London Regional Cancer Program, London Health Sciences Centre, London, ON, Canada, **3** Department of Oncology, Schulich School of Medicine & Dentistry, University of Western University, London, ON, Canada, **4** Cancer Research Laboratories, Lawson Health Research Institute; London, ON, Canada

* alison.allan@lhsc.on.ca

Abstract

Breast cancer is a leading cause of cancer death in women, with the majority of these deaths caused by metastasis to distant organs. The most common site of breast cancer metastasis is the bone, which has been shown to provide a rich microenvironment that supports the migration and growth of breast cancer cells. Additionally, growing evidence suggests that breast cancer cells that do successfully metastasize have a stem-like phenotype including high activity of aldehyde dehydrogenase (ALDH) and/or a $CD44^+CD24^-$ phenotype. In the current study, we tested the hypothesis that these $ALDH^{hi}CD44^+CD24^-$ breast cancer cells interact with factors in the bone secondary organ microenvironment to facilitate metastasis. Specifically, we focused on bone-derived osteopontin and its ability to promote the migration and stem-like phenotype of breast cancer cells. Our results indicate that bone-derived osteopontin promotes the migration, tumorsphere-forming ability and colony-forming ability of whole population and $ALDH^{hi}CD44^+CD24^-$ breast cancer cells in bone marrow-conditioned media (an *ex vivo* representation of the bone microenvironment) ($p \leq 0.05$). We also demonstrate that CD44 and RGD-dependent cell surface integrins facilitate this functional response to bone-derived osteopontin ($p \leq 0.05$), potentially through activation of WNK-1 and PRAS40-related pathways. Our findings suggest that soluble bone-derived osteopontin enhances the ability of breast cancer cells to migrate to the bone and maintain a stem-like phenotype within the bone microenvironment, and this may contribute to the establishment and growth of bone metastases.

Introduction

Breast cancer is the most frequently diagnosed cancer among North American women, currently accounting for approximately 26% of all newly diagnosed cancer cases [1, 2]. Breast cancer's high mortality rate (ranked second among women after lung cancer) is primarily due to the failure of conventional therapy to mitigate and eliminate metastatic disease. While breast

cancer patients with localized disease at the time of diagnosis have an excellent (almost 90%) chance of long-term survival, a patient with metastatic disease has a mere 22% chance of surviving longer than ten years [1, 2].

Although lethal, metastasis is a surprisingly inefficient process, with the rate-limiting steps being the ability to initiate growth after extravasation into the secondary tissue and to maintain that growth into clinically detectable macrometastases [3]. Growing evidence suggests that breast cancer cells that can successfully initiate a primary tumor and traverse the entire metastatic cascade may be "stem-like" cells or so-called "cancer stem cells" (CSCs) because of their unique ability to self-renew and differentiate into a heterogenous tumor [4–7]. These stem-like breast cancer cells can be isolated using specific markers including a CD44+CD24- phenotype and/or high aldehyde dehydrogenase activity (ALDH^{hi}) [8, 9]. Our laboratory has pioneered functional characterization of these cells with regards to metastatic behavior, and were the first to report that stem-like ALDH^{hi}CD44+CD24- cells demonstrate increased proliferation, adhesion, migration and invasion *in vitro* and metastasis *in vivo* relative to their non-stem-like ALDH^{low}CD44-CD24+ counterparts [10].

Clinically, breast cancer metastasizes in an organ-specific pattern to lymph nodes, lung, liver, bone and brain, with the bone being the most common site of metastasis [11–15]. Stephen Paget's seminal "seed and soil" hypothesis, first proposed in 1889, posits that this organ-specific metastatic dissemination is mediated by crosstalk between a subset of cancer cells (the 'seeds') and specific organ microenvironments (the 'soil') [13]. A cancer cell's altered genetic or molecular signature and unique cell surface receptors results in a predilection for certain organ microenvironments, and in turn a favorable niche provides conditions that promote metastatic development [16]. In support of this, a meta-analysis of published autopsy data [12] demonstrated that more bone metastases can be detected in breast cancer patients than would be expected by blood flow alone, indicating that the bone microenvironment is likely very important for metastatic dissemination and growth.

In the context of the CSC hypothesis, the bone microenvironment has been shown to be a rich stem cell niche [17]. Notably, studies have demonstrated that the majority of early-disseminated breast cancer cells found in the bone of breast cancer patients have a stem-like phenotype, an observation that complements the stem cell hypothesis of cancer metastasis [18]. Specifically, breast cancer cells with a CD44+ phenotype have been shown to have increased adherence to human bone marrow endothelial cells [19]. Furthermore, previous studies in our lab have demonstrated that both whole population and ALDH^{hi}CD44+ breast cancer cells show enhanced migration towards bone marrow-conditioned media relative to control [20], although the soluble molecular factors that drive this require further investigation.

Within the bone microenvironment, the acidic phosphoglycoprotein osteopontin (OPN) is the most abundant non-collagenous extracellular matrix protein present, and as such, is a protein of interest when considering the bone as a favorable niche for breast cancer metastases. OPN mediates cell-matrix and cell-cell communication through interactions with a variety of cell surface receptors (i.e. CD44, α9β1, αvβ3 and αvβ5), leading to downstream activation of pathways that ultimately contribute to survival, migration, adhesion, proliferation, angiogenesis, and metastasis [21–24]. Clinically, OPN has been shown to have prognostic value, with observed correlations between plasma OPN levels, metastatic tumor burden and survival in breast cancer patients [25–27]. Although extensive biological research has focused on investigating the functional implications of tumor cell-derived OPN in cancer, the role of bone-derived OPN in the metastatic progression of breast cancer remains poorly understood.

In the current study, we therefore tested the hypothesis that soluble bone-derived OPN plays an important role in the metastatic behavior of breast cancer cells. We demonstrate that

bone-derived OPN promotes the migration and stem-like properties of breast cancer cells via the cell surface receptor CD44 and RGD-dependent cell surface integrins, resulting in activation of WNK-1 and PRAS40. Our findings suggest that soluble bone-derived OPN enhances the ability of breast cancer cells to migrate to bone and maintain a stem-like phenotype within the bone microenvironment, and this may contribute to the establishment and growth of bone metastases.

Materials and methods

Cell culture and reagents

MDA-MB-231 human breast cancer cells [28] were obtained directly from American Type Culture Collection (cat #ATCC-HTB-26; Manassas, VA) and maintained in DMEM/F12 + 10% fetal bovine serum (FBS). SUM159 human breast cancer cells [29] were obtained directly from Asterand Inc. (cat # SUM-159PT, Detroit, MI) and maintained in HAMS:F12 + 5% FBS + 5 μg/mL insulin + 1 μg/mL hydrocortisone + 10mM HEPES. Media/supplements were from Invitrogen (Carlsbad, CA) and FBS was from Sigma-Aldrich (St. Louis, MO). Cell lines were authenticated via third-party testing (IDEXX, Columbia, MO).

Bone-marrow conditioned media

Mice were used for this study. All studies were carried out in strict accordance with the recommendations of the Canadian Council for Animal Care. The protocol was approved by the Animal Care Committee at the University of Western Ontario (protocol# 2009–064). Euthanasia was performed with the use of CO_2 and all efforts were made to minimize suffering. Bone marrow-conditioned media (BMCM) was generated as previously described [20] using bones harvested from healthy female nude mice. Briefly, healthy female nude mice (6–12 weeks old; Hsd: Athymic Nude-Foxn1[nu]; Harlan Sprague-Dawley, Indianapolis, IN) were euthanized and bone marrow was collected by flushing femur cavities. Aspirates were dissociated into single cells by pipetting and cells were washed and plated in DMEM + 10% FBS + penicillin/streptomycin (pen/strep). Resulting adherent bone marrow stromal cells (BMSCs) were passaged 2–3 times, washed, and exposed to DMEM/F12 + Mito[+™] + pen/strep. Conditioned media was collected after 72 hours and stored at -20˚C. To account for mouse-to-mouse variability, BMCM from multiple mice was pooled prior to use.

Protein array analysis

To identify soluble factors present within BMCM, RayBio® AAM-BLM-1 label-based mouse antibody arrays were used to simultaneously assess of expression of 308 soluble murine target proteins (RayBiotech Inc., Norcross, GA) as described previously [20]. Results were visualized using chemiluminescence and film exposure (CL-Xposure Film, Pierce). Densitometric analysis was conducted using Image J with the MicroArray Profile Macro and results (N = 3/media condition) were analyzed using the RayBiotech analysis tool for AAM-BLM-1 as described previously [20]. To identify potential phosphorylation changes in human breast cancer cells in response to BMCM, MDA-MB-231 human cells were incubated in basal media, BMCM, or BMCM depleted of OPN and cell lysates were harvested after 2 hours. Protein concentrations were determined with a DC protein assay (BioRad). Cell lysates were incubated with the Human Phospho-Kinase Array membranes (ARY003B, R&D Systems) overnight at 4˚C. Biotinylated detection antibodies were applied and membranes were visualized using chemiluminescence. Densiotometric analysis was performed using the Protein Array Analyzer for ImageJ (N = 3/ media condition).

Immunodepletion

Osteopontin was immunodepleted from BMCM using a rat anti-mouse OPN-specific antibody (R&D Systems, Burlington, ON). Antibodies were incubated for 20 minutes at room temperature (RT) with Dynabeads Protein G (8 μg OPN-specific antibody per mg of beads; Novex/Life Technologies, Oslo). Bead-antibody complexes were then incubated with BMCM for 30 minutes at RT. Resulting bead-antibody-antigen complexes were removed from BMCM using a DynaMag-2 magnet (Novex/Life Technologies). The concentration of OPN in depleted BMCM was assessed by Quantikine ELISA kits specific for mouse OPN (R&D Systems). Negative controls included BMCM exposed to beads only (no antibody). GST-tagged human OPN (GST-hOPN; a kind gift from Dr. Ann Chambers, London Regional Cancer Program, London, ON [30]) was used for rescue experiments at the same concentration that was originally depleted from BMCM.

Cell migration assays

Transwells® (6.5 mm, 8 μm pore size; Falcon, Corning, NY) were coated with 6 μg of gelatin per well. Osteopontin-depleted, non-depleted BMCM, or basal media was placed in 24-well dishes (n = 3 per condition). MDA-MB-231 or SUM-159 human breast cancer cells (5 x 10^4 cells per well) were plated on top of the gelatin-coated Transwells® and inserted into 24-well dishes. In experiments involving functional blocking of CD44 or RGD, cells were incubated for 30 minutes at RT with rat anti-human CD44 antibody (10 μg per 5 x 10^5 cells; Calbiochem, Mississauga, ON) or an RGD-sequence specific peptide (50 μg per 5 x 10^5 cells for MDA-MB-231 breast cancer cells, 100 μg per 5 x 10^5 cells for SUM-159 breast cancer cells; Sigma-Aldrich). For PI3K/Akt inhibitor experiments, breast cancer cells were first serum-starved for 18 hours, harvested and pretreated for 1 hour with 20 μM of either LY294002 or Triciribine (Millipore, Temecula, CA) or an equivalent concentration of vehicle (DMSO) prior to the migration assay. After 18 hours, Transwells® were fixed and non-migrated cells were removed from the inner surface and migrated cells on the lower surface were stained with DAPI. Five high-powered fields (HPFs) of view were counted for each membrane using ImageJ [National Institutes of Health (NIH), Bethesda, MD] software. Results are expressed as a fold-increase from negative control (N = 3).

Sphere-limiting dilution assays (SLDA) and colony-forming assays

MDA-MB-231 human breast cancer cells were seeded into 96-well plates for colony-forming assays (Corning, Lowell, Massachusetts) or 96-well Ultra-Low Attachment plates (Corning) for the sphere-limiting dilution assay (SLDA) in a serial-diluted fashion ranging from 1000–0.001 cells/well. For functional blocking experiments, anti-CD44 antibody or RGD-sequence specific peptide were used as described for the migration assays. Osteopontin-depleted, non-depleted BMCM, or basal media was added to the wells and cells were cultured for 5 days. At the end of the assay, each well was scored for the presence or absence of colonies or tumor-spheres (N = 3 each) using L-Calc™ Software (Stem Cell Technologies, Vancouver, BC).

Fluorescence-activated cell sorting (FACS) and flow cytometry

$ALDH^{hi}CD44^+CD24^-$ and $ALDH^{lo}CD44^-CD24^+$ cells subpopulations were isolated from the MDA-MB-231 human breast cancer cell line as described previously [10, 31]. Briefly, cells were concurrently labeled with 7-amino-actinomycin D (7-AAD), ALDEFLUOR™ assay kit (StemCell Technologies; Vancouver, BC) and fluorescently-conjugated antibodies including anti-CD44 (clone IM7) conjugated to allophycocyanin (APC) and anti-CD24 (clone ML5)

conjugated to phycoerytherin (PE) (BD Biosciences). ALDH activity was used as the primary sort criteria (top ~20% = ALDH^{hi}; bottom ~20% = ALDH^{low}) and CD44^{+}CD24^{-} phenotype as the secondary sort criteria (top ~10% gated on ALDH^{hi}; bottom ~10% gated on ALDH^{low}). Cell viability was assessed by 7-AAD staining during cell sorting, and confirmed by trypan blue exclusion post-sorting. FACS-isolated cells were used immediately for *in vitro* assays.

For flow cytometry analysis, MDA-MB-231 and SUM159 human breast cancer cells were grown to 80% confluence in normal growth media, harvested and resuspended at 1 x 10^{6} cells/ml. Cells were then incubated with phycoerytherin (PE)-conjugated CD44 (BD Biosciences, San José, CA), fluorescein isothiocyanate (FITC)-conjugated αvβ3 (R&D Systems), Alexafluor (AF)-488-conjugated αvβ5 (R&D Systems), AF-488-conjugated β1 (R&D Systems) or AF-488-conjugated α9β1 (R&D Systems) antibodies for 1 hour at 4°C. Negative controls included cells only (no antibody) and cells incubated with an isotype-matched IgG-control. Samples were analyzed on a Beckman-Coulter EPICS XL-MCL flow cytometer.

Immunoblotting

MDA-MB-231 human cells were incubated in basal media, BMCM, or BMCM depleted of OPN and cell lysates were harvested after 2 hours. Protein concentrations were determined with a DC protein assay (BioRad). Immunoblotting was used to assess the expression of total PRAS40 (anti-human PRAS40 [Clone 660928], R&D Systems), phosphorylated PRAS40 (anti-human Phospho-PRAS40 [T246] [Clone 760502], R&D Systems), total WNK-1 (anti-human polyclonal Ab, Cell Signaling), or phosphorylated WNK-1 (anti-human Phospho-WNK1 [T60] polycolonal, R&D Systems). β-actin was used as a loading control (anti-human anti-ACTB [SAB2108641], Sigma).

siRNA targeting of WNK1 and PRAS40

For knockdown of WNK1 and PRAS40, ON-TARGETplus SMART pools of 4 specific or control small interfering RNAs (siRNA) (Dharmacon Thermo Scientific, Lafayette, CO) were used in combination with transient transfection of MDA-MB-231 human breast cancer cells. All siRNAs were suspended in sterile RNAse-free water at a concentration of 25 μM. Scrambled control, WNK1, or PRAS40 siRNA pools (6ul) and 10ul Lipofectamine RNAiMAX reagent (Invitrogen) were diluted into serum-free Opti-MEM media (Invitrogen) and incubated for 20 min at room temperature before addition to MDA-MB-231 cells (50% confluency) in 60 mm culture dishes. After 48 hours of incubation at 37°C, 5% C0$_2$, cells were harvested, assessed for knockdown efficiency by immunoblotting and used for migration assays as described above.

Data analysis

In vitro experiments were performed a minimum of three times with three technical replicates within each experiment. Unless otherwise noted, data are presented as mean ± SEM. Statistical analysis was performed using GraphPad Prism 6.0 (GraphPad Software, San Diego, CA) using one-way analysis of variance (ANOVA) with Tukey's or Bonferroni's post-hoc tests. In all cases, values of $p < 0.05$ were classified as being statistical significant.

Results

Soluble OPN is produced in the bone microenvironment and enhances breast cancer cell migration

An initial investigation of potential soluble factors present in the bone microenvironment was carried out using protein array analysis of bone marrow-conditioned media (BMCM) as a

model system [20]. Of the proteins identified in BMCM, several were found to be associated with metastasis, including the soluble phosphoprotein osteopontin (OPN) (S1 Table). In the current study, we chose to focus our work on OPN because of its established function in both the normal bone microenvironment and during breast cancer metastasis [21–24]. ELISA analysis demonstrated that that BMCM contains significant amounts of bone-derived OPN compared to basal media (P≤0.05; Fig 1A). To assess the effect of bone-derived OPN on human breast cancer cell migration, OPN was immunodepleted from BMCM. Transwell™ migration assays were then used to assess the migration of MDA-MB-231 and SUM-159 human breast cancer cells to basal media, BMCM and BMCM depleted of OPN. Both cell lines exhibited increased migration toward BMCM relative to basal media (P≤0.05; Fig 1B and 1C) and exhibited significantly decreased migration to BMCM depleted of OPN, back down to levels comparable to basal media (P≤0.05; Fig 1B and 1C). To validate that bone-derived OPN was specifically responsible for the observed effects on breast cancer cell migration, recombinant human OPN (GST-hOPN) was added back into BMCM depleted of OPN at the same concentration that was originally depleted. The addition of GST-hOPN to BMCM rescued the migratory effect on both MDA-MB-231 and SUM-159 cells, causing cells to migrate at similar levels as non-depleted BMCM (Fig 1B and 1C). These results demonstrate that bone-derived OPN enhances breast cancer cell migration towards BMCM.

Bone-derived OPN enhances the migration and stem-like behavior of ALDH^{hi}CD44^{+}CD24^{-} breast cancer cells

As previously discussed, "stem-like" ALDH^{hi}CD44^{+}CD24^{-} breast cancer cells show enhanced metastasis to multiple different organs, including bone [7, 10]. We have previously shown that this subpopulation is found within the MDA-MB-231 cell line and shows increased migration to BMCM relative to ALDH^{lo}CD44^{-}CD24^{+} cells [20]. Thus, we wanted to investigate if bone-derived OPN influenced the migration of this population. Using FACS, ALDH^{hi}CD44^{+}CD24^{-} and ALDH^{lo}CD44^{-}CD24^{+} subpopulations were isolated from the MDA-MB-231 cell line using the strategy outlined in S1 Fig and used in migration assays in combination with basal media, BMCM, or BMCM depleted of OPN. The ALDH^{hi}CD44^{+}CD24^{-} subpopulation demonstrated significantly increased migration toward BMCM compared to basal media, an effect that was abrogated when OPN was depleted from BMCM (P≤0.05; Fig 2A). In contrast, ALDH^{lo}CD44^{-}CD24^{+} cells did not display significantly increased migration towards either BMCM or BMCM depleted of OPN compared to basal media (P>0.05; Fig 2A).

Next, we used a sphere limiting dilutions assay (SLDA) to assess the effect of bone-derived OPN on the tumorsphere-forming capacity of breast cancer cells. Whole population MDA-MB-231 cells demonstrated increased tumorsphere-forming capacity in BMCM compared to basal media (P≤0.05; Fig 2B). This tumorsphere-forming ability decreased when BMCM was depleted of OPN (P≤0.05; Fig 2B), suggesting that bone-derived OPN supports this capacity in MDA-MB-231 cells. Additionally, the tumorsphere-forming ability of ALDH^{hi}CD44^{+}CD24^{-} cells was reduced in the presence of BMCM depleted of OPN relative to BMCM (P≤0.05; Fig 2C), indicating that this cell subpopulation is responsible for the tumorsphere-forming capacity of MDA-MB-231 cells in BMCM and that bone-derived OPN supports their stem-like phenotype. We also investigated the influence of bone-derived OPN on the colony-forming ability of MDA-MB-231 cells. Whole population MDA-MB-231 cells show increased colony-forming abilities in BMCM compared to basal media (P≤0.05; Fig 2D). When cells were exposed to BMCM depleted of OPN, their colony-forming capacity was significantly reduced (P≤0.05; Fig 2D), suggesting that bone-derived OPN also plays a role in the colony-forming ability of breast cancer cells.
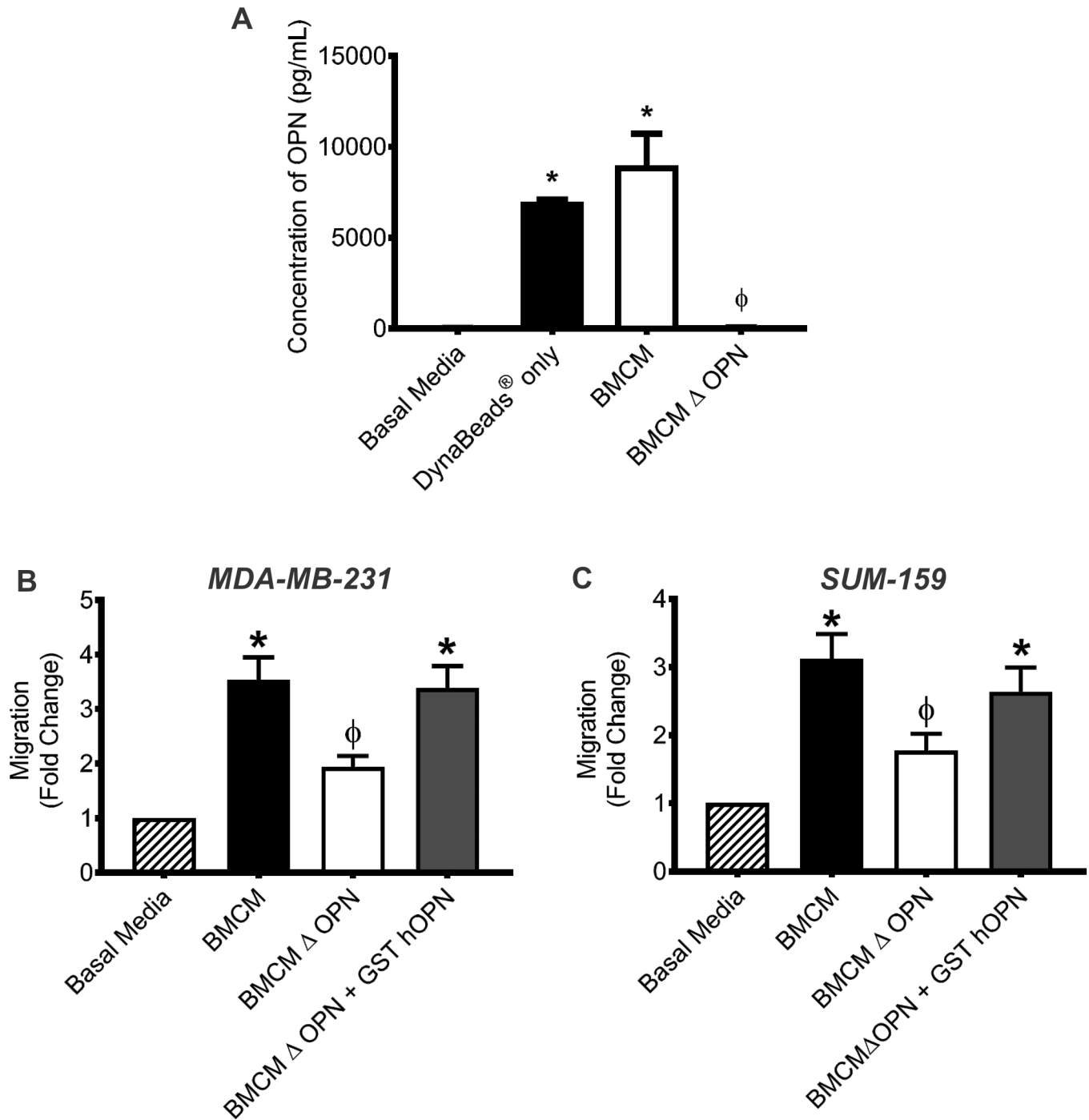
Fig 1. Soluble OPN is produced in the bone microenvironment and enhances human breast cancer cell migration. (A) Goat anti-mouse OPN primary antibody was incubated for 20 min at RT with DynaBeads® Protein G prior to incubation with BMCM for 30 min at RT. The beads-antibody-antigen complex was removed with a DynaMag™-2 magnet. Concentration of OPN in BMCM, BMCM with beads only (no antibody) and BMCM depleted of OPN (ΔOPN) was assessed by ELISA. Data are presented as mean ± SEM (N = 3). (B) MDA-MB-231 and (C) SUM-159 cells were subjected to transwell migration assays (5 x 10^4 cells/well; 8μm pore size) using basal media (DMEM/F12 + Mito+), BMCM, BMCM depleted of OPN (ΔOPN) or BMCM ΔOPN rescued with GST-hOPN. Plates were incubated at 37°C, 5% CO_2 for 18 hr, fixed and stained. Five high-powered fields of view (HPF) were captured per transwell and migrated cells were analyzed. Data are presented as mean ± SEM (N = 3; fold-change from negative control basal media). * = significantly different than basal media; φ = significantly different than BMCM (P≤0.05).
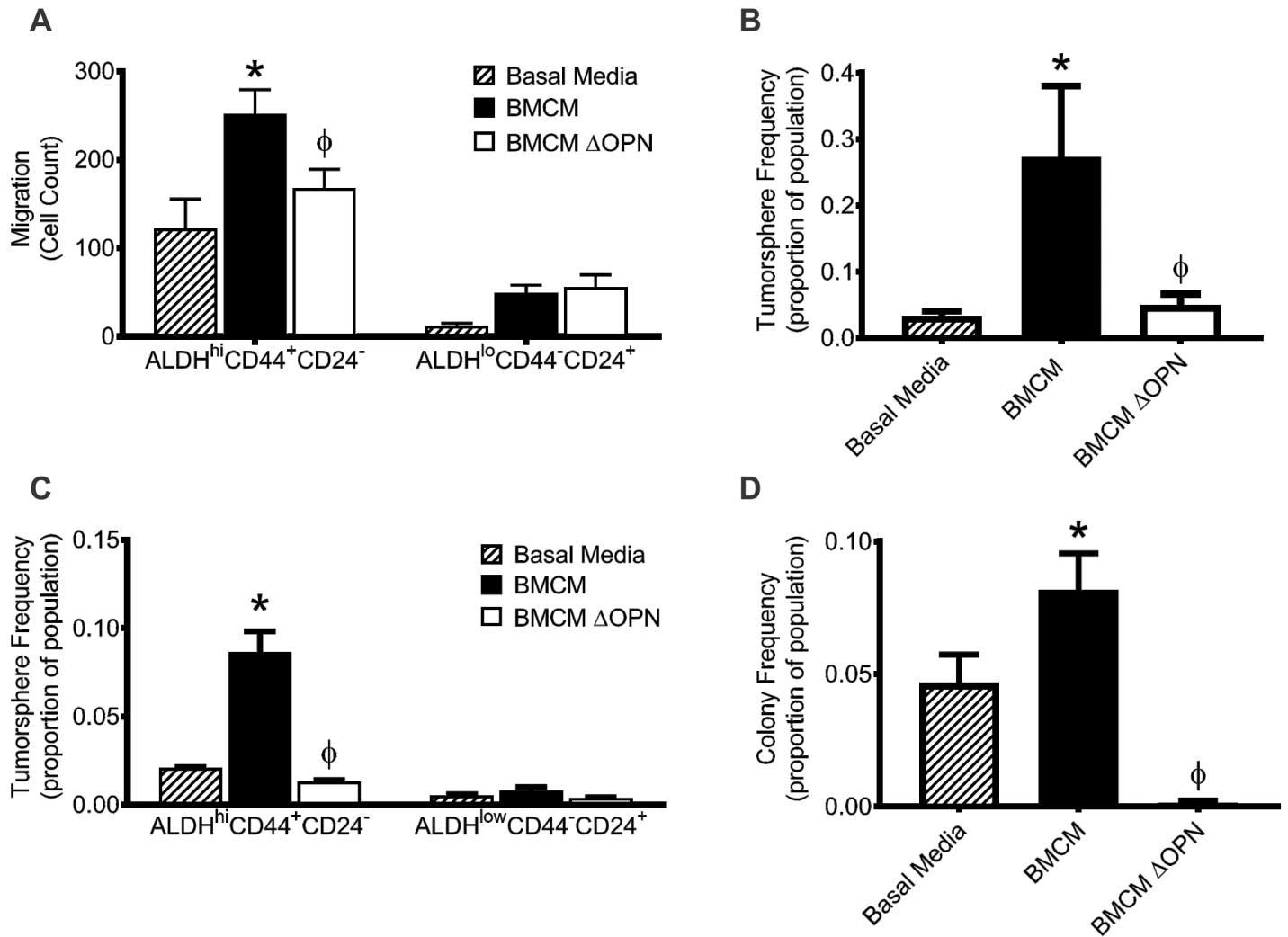
Fig 2. Bone-derived OPN enhances the migration and stem-like behavior of ALDH^{hi}**CD44**$^{+}$**CD24- breast cancer cells.** (A) ALDH^{hi}CD44^{+}CD24^{-} and ALDH^{lo}CD44^{-}CD24^{+} cell subpopulations were isolated from the MDA-MB-231 human breast cancer cell line by FACS and subjected to transwell migration assays (5 x 10^{4} cells/well; 8μm pore size) using basal media (DMEM/F12 + Mito^{+}), BMCM, or BMCM depleted of OPN (ΔOPN). Plates were incubated at 37˚C, 5% CO$_2$ for 18 hr, fixed and stained. Five high-powered fields of view (HPF) were captured per transwell and migrated cells were analyzed. (B) Whole population or (C) ALDH^{hi}CD44^{+}CD24^{-} and ALDH^{lo}CD44^{-}CD24^{+} subpopulations isolated from the MDA-MB-231 breast cancer cell line were plated in a limiting dilution fashion on 96-well ultra-low attachment plates for 7 days in basal media, BMCM, or BMCM ΔOPN and subjected to sphere-forming assays. (D) Whole population MDA-MB-231 cells were plated in a limiting dilution fashion on normal 96-well plates for 7 days in basal media, BMCM, or BMCM ΔOPN and subjected to colony-forming assays. Data are presented as mean ± SEM (N = 3). * = significantly different than basal media; ϕ = significantly different than BMCM (P≤0.05).

https://doi.org/10.1371/journal.pone.0177640.g002

Bone-derived OPN interacts with CD44 and RGD-dependent integrins to enhance migration

OPN is known to influence multiple steps in the metastatic cascade through the cell surface receptor CD44, as well as multiple different cell surface integrins; including αvβ1, α9β1 αvβ3 and αvβ5 [21]. Thus, we first evaluated the expression of CD44, β1, α9β1 αvβ3 and αvβ5 on the MDA-MB-231 and SUM-159 cell lines. Flow cytometry indicated that both cell lines are positive for the expression of CD44 and these four cell surface integrins (S2 and S3 Figs). Next, we investigated the role of these cell surface proteins in the migration of breast cancer cells using an anti-CD44 functional blocking antibody or an Arg-Gly-Asp (RGD) peptide. OPN

contains an RGD sequence that is recognized by β1, α9β1 αvβ3 and αvβ5 integrins; therefore incubating the cells with the RGD-sequence specific peptide prior to use in functional assays should block the recognition of OPN via the RGD sequence [30, 32].

We observed that blocking CD44 on the MDA-MB-231 and SUM-159 cells significantly decreased migration to BMCM compared to migration of untreated cells (P≤0.05; Fig 3A and 3B). The migration of CD44-blocked MDA-MB-231 cells to BMCM was only reduced to a level similar to untreated cells exposed to BMCM depleted of OPN, suggesting that CD44 specifically contributes to the effect of bone-derived OPN on breast cancer cell migration (P>0.05; Fig 3A). In contrast, CD44-blocked SUM-159 cell migration to BMCM was significantly lower than untreated SUM-159 cell migration to BMCM depleted of OPN (P≤0.05; Fig 3B). This suggests that CD44 may mediate the interaction of SUM-159 with bone-derived OPN as well as other soluble factors within BMCM.

Our results also indicate that treatment of MDA-MB-231 and SUM-159 breast cancer cells with a RGD-blocking peptide significantly reduces their migration to BMCM relative to untreated cells (P≤0.05; Fig 3C and 3D). RGD-blocked MDA-MB-231 cells showed significantly decreased migration to BMCM compared to untreated cells exposed to BMCM depleted of OPN (P≤0.05; Fig 3C). These results suggest that RGD-dependent integrins may mediate the interaction of MDA-MB-231 with bone-derived OPN as well as other soluble factors within the BMCM. In contrast, RGD-blocked SUM-159 cells showed similar migratory levels to BMCM as untreated cells to BMCM depleted of OPN, suggesting that RGD-dependent cell surface integrins specifically mediate the interaction of SUM-159 cells with bone-derived OPN (P>0.05; Fig 3D).

Promotion of breast cancer cell stem-like behavior by bone-derived OPN is mediated through CD44 and RGD-dependent integrins

Given that CD44 and RGD-dependent integrins mediate the interaction between breast cancer cells and bone-derived OPN to influence migration to BMCM, we wanted to explore if these cell surface receptors also influence the stem-like phenotype of breast cancer cells. The anti-CD44 blocking antibody and RGD-sequence specific peptide were used to block MDA-MB-231 in the SLDA. Both CD44-blocked and RGD-blocked MDA-MB-231 cells showed decreased tumorsphere-forming capacity when exposed to BMCM and BMCM depleted of OPN compared to untreated cells exposed to BMCM depleted of OPN (P≤0.05; Fig 4A and 4B). This suggests that both CD44 and RGD-dependent integrins can mediate the tumorsphere-forming capacity of breast cancer cells through interactions with OPN.

Bone-derived OPN induces phosphorylation of WNK1 and PRAS40

Thus far, we have shown that bone-derived OPN influences the migratory ability and stem-like phenotype of breast cancer cells via CD44 and RGD-dependent integrins. Considering this, we wanted to investigate the effect of bone-derived OPN on downstream pathways within breast cancer cells. MDA-MB-231 cells were exposed to basal media, BMCM, or BMCM depleted of OPN. Cell lystates were collected after 2 hours and assessed using human phospho-kinase arrays. We observed that phosphorylation of WNK1, PRAS40, and HSP60 increased after exposure to BMCM, and this phosphorylation was abrogated when OPN was depleted (Fig 5A). We were able to validate these findings for PRAS40 (Fig 5B) and WNK1 (Fig 5C) using immunoblotting, but not HSP60. These findings indicate that bone-derived OPN leads to phosphorylation of WNK1 and PRAS40 and suggests that activation of these pathways may be a potential contributing mechanism underlying the functional role of bone-derived OPN in the malignant behavior of breast cancer cells.
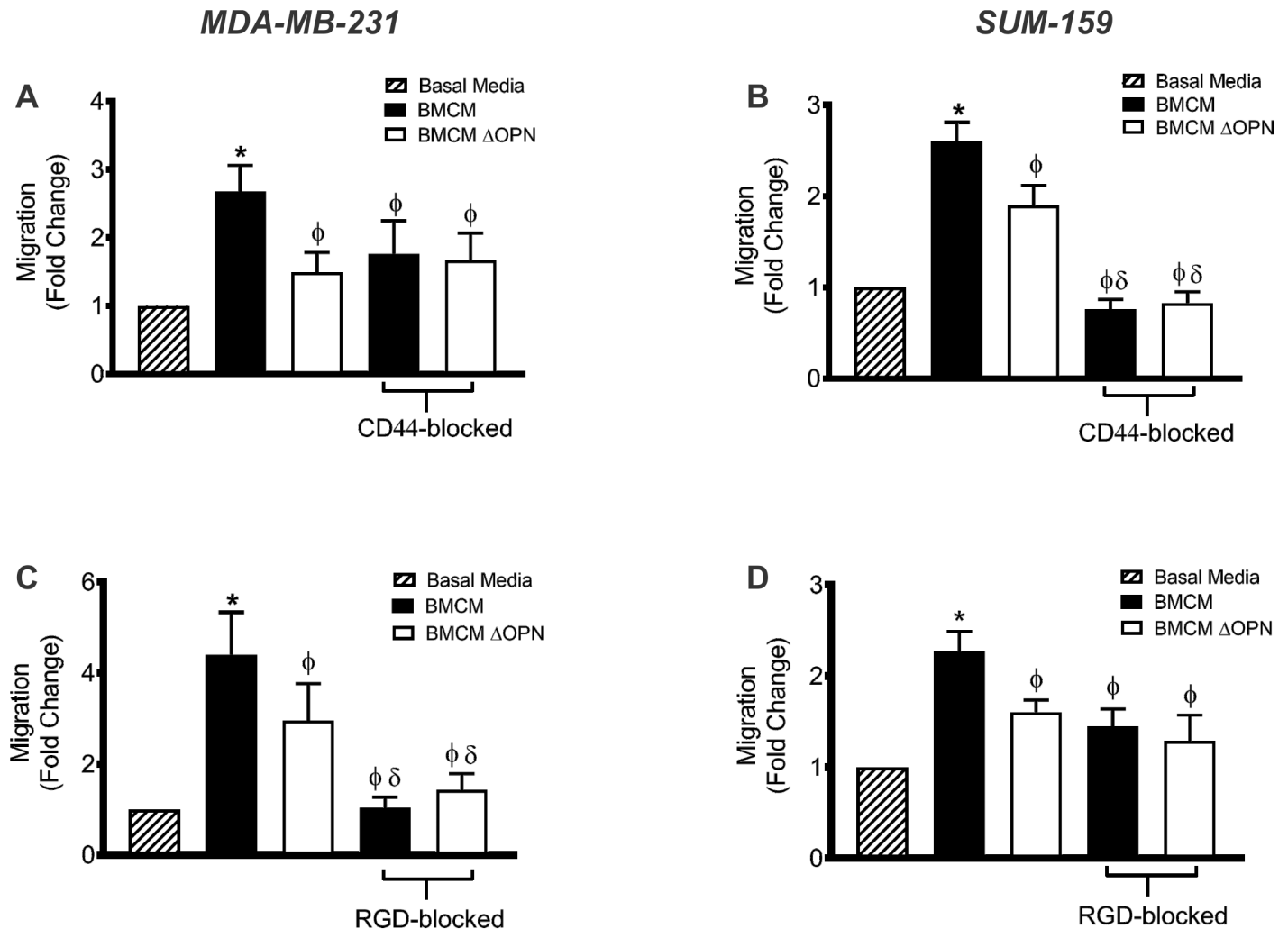
MDA-MB-231

SUM-159

Fig 3. Bone-derived OPN interacts with CD44 and RGD-dependent integrins to enhance breast cancer cell migration. MDA-MB-231 and SUM-159 human breast cancer cells were blocked with an anti-CD44 antibody (A, B) or an RGD sequence-specific blocking peptide (C, D) for 30 min and subjected to transwell migration assays (5 x 10^4 cells/well; 8μm pore size) using basal media (DMEM/F12 + Mito+), BMCM, or BMCM depleted of OPN (ΔOPN). Plates were incubated at 37˚C, 5% CO_2 for 18 hr, fixed and stained. Five high-powered fields of view (HPF) were captured per transwell and migrated cells were analyzed. Data are presented as mean ± SEM (N = 3; fold change from negative control of basal media). * = significantly different than basal media; φ = significantly different than non-blocked BMCM, δ = significantly different than non-blocked BMCM ΔOPN (P≤0.05).

https://doi.org/10.1371/journal.pone.0177640.g003

WNK1 and PRAS40-related pathways play a role in BMCM-mediated migration of breast cancer cells

To explore the potential role of these factors further, we directly targeted WNK1 and PRAS40 using siRNA. We observed that knockdown of WNK1 resulted in a significant reduction of breast cancer cell migration in response to BMCM relative to a non-specific siRNA control (Fig 6A; P≤0.05). In contrast, knockdown of PRAS40 had no effect on BMCM-mediate breast cancer cell migration (Fig 6B). Since PRAS40 is downstream of both PI3K and Akt [33], we hypothesized that its activation and effect on migration was indirectly related to the activity of one of these pathways. We observed that treatment with the PI3K inhibitor LY294002 resulted in a significant reduction of breast cancer cell migration in response to BMCM (Fig 6C; P≤0.05), whereas treatment with the Akt inhibitor Triciribine or a vehicle control had no effect (Fig 6C).
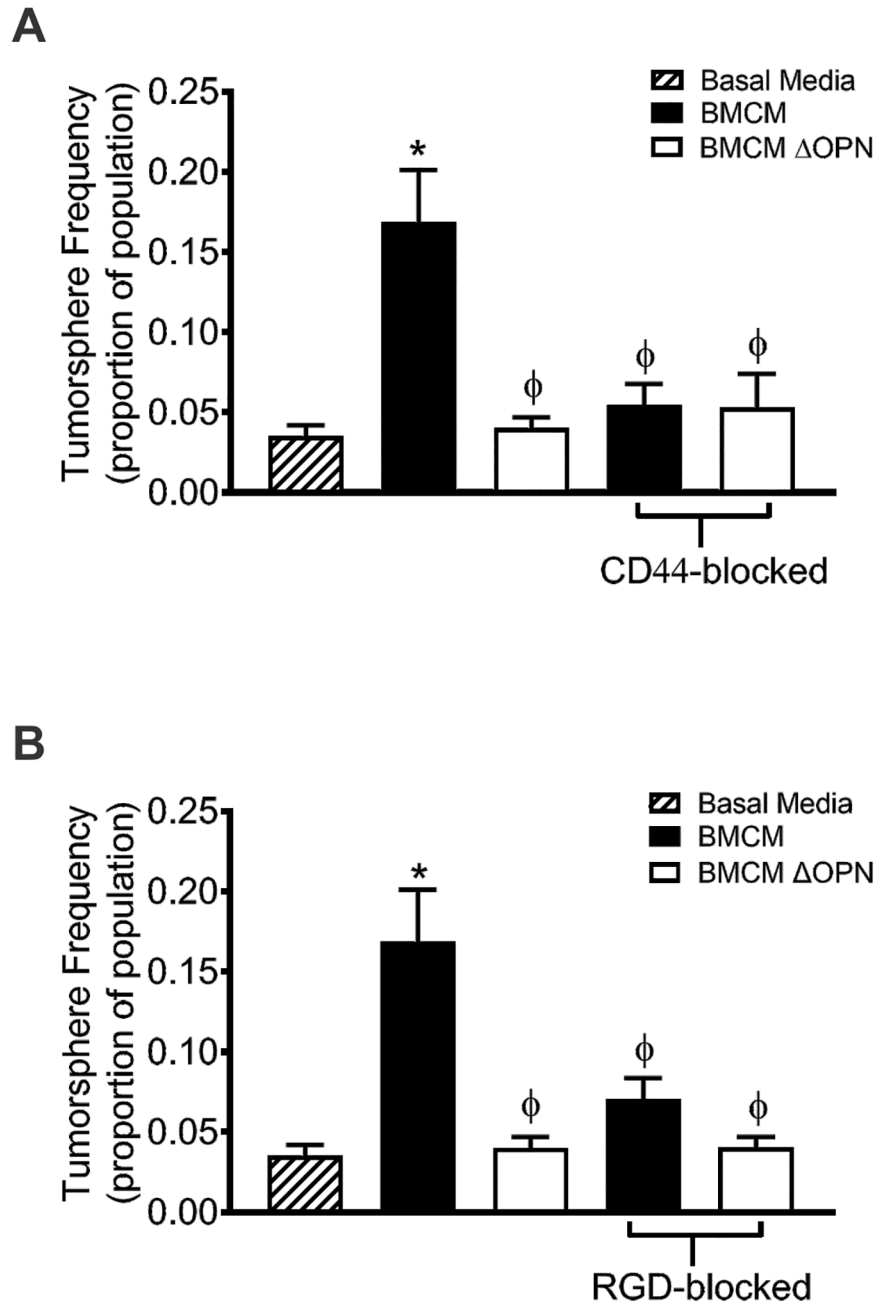
Fig 4. Breast cancer cell stem-like behavior is mediated by bone-derived OPN through CD44 and RGD-dependent integrins. MDA-MB-231 human breast cancer cells were blocked with (A) an anti-CD44 antibody or (B) an RGD sequence-specific blocking peptide for 30 minutes prior to plating in a limiting dilution fashion on ultra-low adhesion 96-well plates for 7 days in basal media (DMEM/F12 + Mito$^+$), BMCM or BMCM ΔOPN in the sphere limiting dilution assay (SLDA). Data are presented as mean ± SEM (N = 3; fold change from negative control of basal media). * = significantly different than basal media; ϕ = significantly different than non-blocked BMCM (P≤0.05).

https://doi.org/10.1371/journal.pone.0177640.g004

Discussion

Approximately 85% of all breast cancer patients who die from their disease are expected to show metastasis to the bone [34]. These bone metastases pose an extreme burden for breast
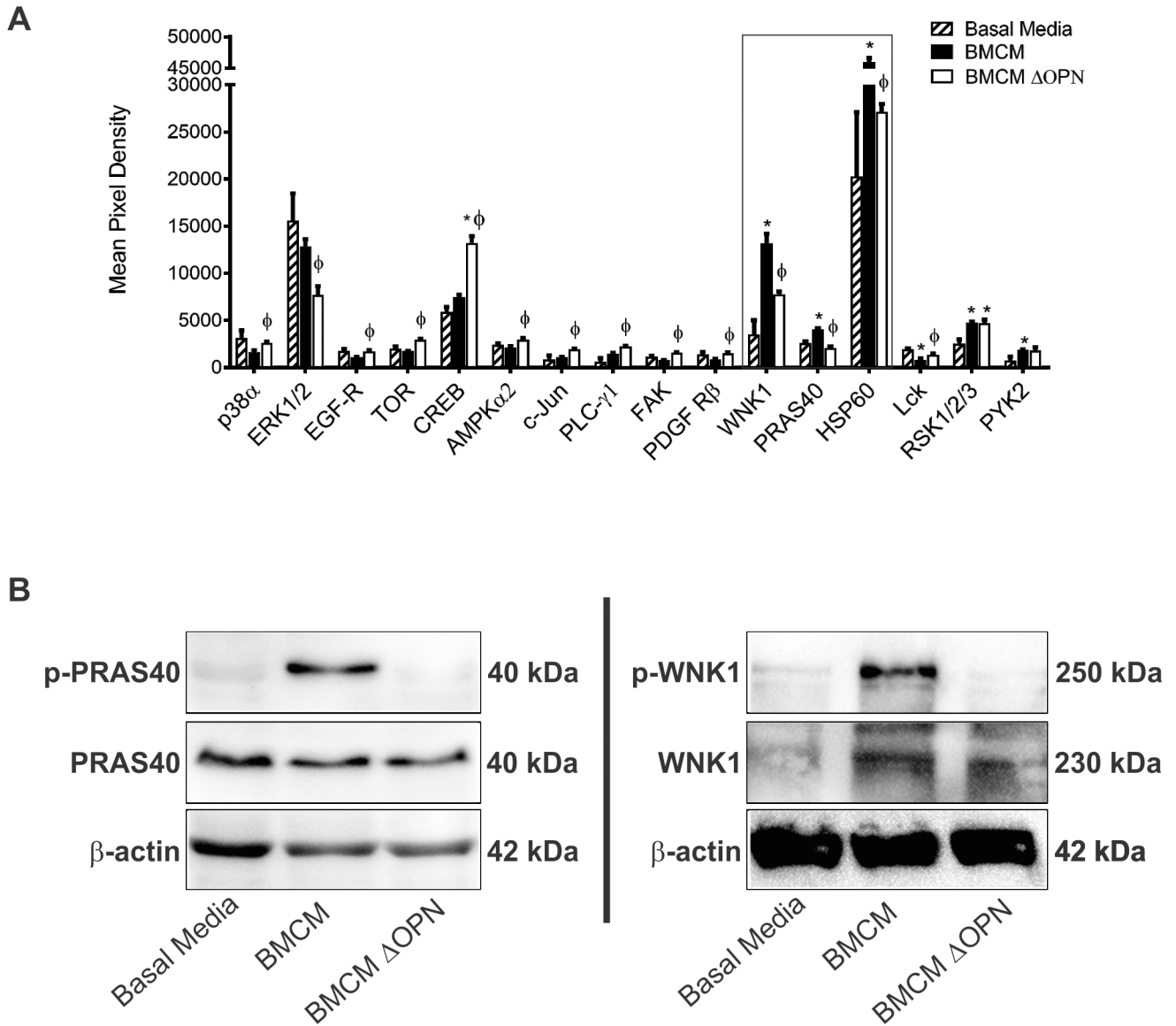
Fig 5. Bone-derived OPN induces phosphorylation of WNK1 and PRAS40. MDA-MB-231 human breast cancer cells were exposed to basal media, BMCM and BMCM depleted of OPN (BMCM ΔOPN) for 2 hours, and cell lysates were harvested. (A) Cell lysates were assessed using with Human Phospho-Kinase Array membranes (ARY003B, R&D Systems) overnight at 4˚C. Biotinylated detection antibodies were applied and membranes were visualized using chemiluminescence. Densitometry analysis was performed using the Protein Array Analyzer for ImageJ (N = 3 for each media condition). * = significantly different than basal media; ϕ = significantly different than BMCM (P≤0.05). Only proteins with significantly different phosphorylation or expression between at least two treatments are shown. Proteins within the rectangular box demonstrated a similar pattern of phosphorylation to each other (increase in response to BMCM, with a subsequent decrease upon depletion of bone-derived OPN). (B) Phosphorylation patterns for PRAS40 and WNK1 were successfully validated using immunoblotting (N = 3).

cancer patients, resulting in pain, fractures and hypercalcaemia, and the current clinical management for metastatic patients fails to prevent or cure these skeletal lesions [34].

The frequency of bone metastases in patients suggests that the bone microenvironment is conducive to the migration and growth of breast cancer cells [35]. Many previous studies have focused on the contribution of breast cancer cell-specific genes, receptors and secreted factors that contribute to the establishment of bone metastases in breast cancer patients. For example,

Fig 6. WNK1 and PRAS40-related pathways play a role in BMCM-mediated migration of breast cancer cells. (A, B) MDA-MB-231 human breast cancer cells were subjected to siRNA knockdown of WNK1 (A) or PRAS40 (B). Knockdown was confirmed by immunoblotting (top panels) prior to carrying out transwell migration assays (bottom panels; 5 x 10⁴ cells/well; 8μm pore size) using basal media (DMEM/F12 + Mito⁺) or BMCM. (C) MDA-MB-231 human breast cancer cells were serum-starved and treated with 20μM of PI3K inhibitor (LY294002) or Akt inhibitor (Triciribine) or an equivalent concentration of vehicle (DMSO) for 1 hour before being subjected to transwell migration assays (5 x 10⁴ cells/well; 8μm pore size) using basal media (DMEM/F12 + Mito⁺) or BMCM. Plates were incubated at 37°C, 5% CO₂ for 18 hr, fixed, and stained. Five high-powered fields of view

(HPF) were captured per transwell and migrated cells were analyzed. Data are presented as mean ± SEM (N = 3; fold change from negative control of basal media). * = significantly different than basal media; φ = significantly different than BMCM + siCON (A, B) or BMCM + vehicle (C) (P≤0.05).

there exists in the literature a wide breadth of knowledge on the effect of tumor-derived OPN in multiple steps of the metastatic cascade [24, 36–46]. However, much less research has been conducted on the effect of host-derived OPN in the tumor microenvironment. The current study focused on elucidating the role of bone-derived OPN on the migration, stem-like behavior and downstream signaling response of breast cancer cells.

We first demonstrated that OPN promotes the migration of breast cancer cells toward bone-marrow conditioned media. Taken together with previous work demonstrating that OPN-deficient mice display less colonization and growth of injected melanoma cells in bone than wild-type mice [47], this data suggests that bone-derived OPN increases breast cancer cell migration to and colonization in bone, thus promoting breast cancer bone metastases. Interestingly, both human breast cancer cell lines used in this study (MDA-MB-231 and SUM-159) displayed reduced migration towards BMCM depleted of OPN compared to non-depleted BMCM. However, levels of migration toward BMCM depleted of OPN were still significantly higher than migration toward basal media, suggesting that other factors within the BMCM may be contributing to the migration of these cancer cells. We identified other soluble factors present within the BMCM that could be responsible for the observed effect, including matrix-metalloproteinase-14 (MMP-14; MTI-MMP) and intracellular adhesion molecule-1 (ICAM-1), and these require further investigation.

Our results also suggest a novel function for bone-derived OPN in promoting the tumor-sphere and colony-forming abilities of breast cancer cells. Sphere-limiting dilution assays (SLDA) and colony-forming assays were used assess the number of tumorsphere-initiating cells present in populations and the ability of cells to proliferate into colonies at very low numbers, which taken together can help evaluate the "stemness" of a population *in vitro* [48].

In healthy tissues, normal stem cells reside in specialized niches that influence their ability to remain quiescent, self-renew or differentiate via cell-to-cell interactions and/or via response to various secreted soluble factors and extracellular matrix components [49, 50]. The bone marrow is known to provide a rich stem cell niche, particularly for hematopoietic stem cells (HSCs) [49, 51] and OPN has recently been shown to be integral in supporting the HSC niche in bone by promoting the migration and lodging of HSCs within the bone endosteal region [52]. Similar to healthy stem cells within the normal bone marrow niche, stem-like cancer cells have also been shown to be influenced and maintained by components of the microenvironment in which they reside, such as stromal cells and soluble factors [53]. Recent work has implicated OPN in the maintenance of "stemness" in different types of cancers. Pietras et al (2014) showed that OPN was able to promote stemness in proneural glioblastoma [54], and Cao et al (2015) showed that OPN promotes a cancer stem cell-like phenotype in hepatocellular carcinoma cells. The ability of bone-derived OPN to maintain the stem-like behavior of breast cancer cells *in vitro* suggest that it may also support the establishment of breast cancer metastases in the bone *in vivo*.

Given our work showing that bone-derived OPN promotes the migration and stem-like behavior of breast cancer cells, we wanted to investigate which cell surface receptors bone-derived OPN uses to influence breast cancer cell properties, and we chose to evaluate the role of CD44 and RGD-dependent integrins in these functions. CD44 plays an important role in metastasis by participating in a variety of signaling networks that promote migration, invasion, growth and survival [55] and our lab has recently showed that breast cancer cells preferentially migrate toward lung-derived OPN in a CD44-dependent manner [20]. RGD-dependent cell

surface integrins (α5β1, α8β1 and all αv-containing integrins) assist in adhesion and migration by recognizing ligands that contain the RGD motif (Arg-Gly-Asp), mainly found in components of the extracellular matrix such as OPN, fibronectin, and vitronectin [56].

Our results show that blocking CD44 or RGD-dependent integrins on the surface of breast cancer cells abrogates migration toward BMCM. Interestingly, we found cell line-specific migratory responses when the OPN-CD44 or the OPN-RGD interactions are blocked. MDA-MB-231 cells seem to be more dependent on CD44 versus RGD integrins for their response to bone-derived OPN; whereas SUM-159 cells depend more heavily on RGD integrins for this response. Flow cytometry analysis revealed that both cell lines express significant amounts of CD44 and similarly moderate amounts of RGD-dependent β1, αvβ3 and αvβ5 and RGD-independent α9β1, suggesting that the differences in migratory function observed could be dependent on the expression of other cell surface receptors including integrins such as α5β1 and α8β1.

Finally, we wanted to begin to explore the downstream signaling pathways that OPN activates to influence breast cancer cell properties and functions. We observed that bone-derived OPN specifically promoted the phosphorylation of WNK-1 and PRAS40, and that these pathways are important for mediating the migration of breast cancer cells in response to BMCM. WNK1 is a seronine-threonine protein kinase that is involved in the MAPK cascade and in EGF-dependent stimulation of ERK1/2 and ERK5 [57, 58]. Previous studies have shown that knockdown of WNK1 in leads to the suppression of ERK1/2 by EGF and results in reduced cell growth and migration [57]. WNK1 is also known suppress TGF-β signaling. TGF-β is integral in inducing the epithelial-to-mesenchymal transition (EMT) thus loss or inactivation of WNK1 activity could promote EMT of epithelial tumor cells [59]. WNK1 is linked to Rho GTPases, which control the dynamics of the cytoskeleton and are integral in cell migration and invasiveness [60, 61]. Our data support this role for WNK1, as knockdown of WNK1 resulted in reduced migration of breast cancer cells in response to BMCM. WNK1 is also a substrate of Akt, suggesting that it may play a role in the PI3K/Akt pathway [58]. Its role in this pathway could cause WNK1 to be indirectly phosphorylated by the interaction of bone-derived OPN with αvβ3 on breast cancer cells, and thus could contribute to breast cancer migration, invasiveness and cell growth downstream of OPN. PRAS40 is a proline-rich substrate of Akt and mTORC1 that acts at the intersection of the Akt and mammalian target of rapamycin (mTOR) signaling pathways. The expression of phospho-PRAS40 is upregulated in 40% of primary breast cancer samples and correlates with PI3K-Akt signaling and activation [33]. Based on our results, it is likely that bone-derived OPN causes phosphorylation of PRAS40 indirectly by activating the PI3K pathway since OPN signals through this pathway via αVβ3 to promote migration, invasion, cell survival and proliferation [62]. While experimental studies have demonstrated a role for the PI3K pathway in bone metastasis of breast cancer [63, 64], to the best of our knowledge neither WNK1 or PRAS40 have previously been specifically implicated in bone metastasis. Our results support the need for future studies aimed at a detailed investigation of the role of these pathways and their potential as therapeutic targets for breast cancer bone metastasis.

In conclusion, this study shows that bone-derived OPN promotes the migration of breast cancer cells and contributes to maintaining the stem-like behavior of breast cancer cells through interactions with CD44 and RGD-dependent integrins. This study also shows that bone-derived OPN activates a downstream signaling response in breast cancer cells involving the phosphorylation of WNK-1 and PRAS40, and that these pathways contribute to enhanced migration of breast cancer cells in the context of the soluble bone microenvironment. While the cancer research community has known about specific metastatic patterns and organ preferences that breast cancers exhibit for over a century, only recently have efforts focused on the

role of the secondary site or "soil" in promoting and supporting metastatic growth at these sites. It is becoming increasingly clear that the bone microenvironment offers an optimal niche for the establishment and progression of metastases. Our study shows that bone-derived soluble factors–specifically OPN–contribute to this process, possibly by interacting with stem-like breast cancer cells. Future studies should concentrate on further elucidating the crosstalk between the "seed" and "soil" during metastasis as this knowledge could direct the development of novel therapeutics aimed at preventing and treating metastasis.

Supporting information

S1 Fig. Strategy for isolation of ALDH^{hi}CD44$^+$CD24$^-$ and ALDH^{lo}CD44$^-$CD24$^+$ breast cancer cell subpopulations. MDA-MB-231 human breast cancer cells were labeled with anti-CD44-APC, anti-CD24-PE, the ALDEFLUOR^{TM} assay kit, and 7-AAD viability dye. Cell subsets were isolated using a four-colour protocol on a FACS ARIA III. (A) Cells were first isolated based on expected light scatter and then (B) viability based on 7-AAD exclusion. (C) Cells are then analyzed for ALDH activity; the top 20% most positive for ALDH activity are deemed ALDH^{hi} and the bottom 20% for lowest ALDH activity are deemed ALDH^{lo}. (D) ALDH^{hi} cells are selected for CD44$^+$/CD24$^-$ phenotype and (E) ALDH^{lo} cells are selected for CD44$^-$/CD24$^+$ phenotypes.
(TIF)

S2 Fig. MDA-MB-231 human breast cancer cells express CD44 and multiple different cell surface integrins. Representative histograms are shown from flow cytometry characterization of MDA-MB-231 cells incubated with (A) PE-conjugated anti-CD44, (B) AlexaFluor-488-conjugated anti-β1 integrin, (C) FITC-conjugated anti-αvβ3 integrin, (D) AlexaFluor-488-conjugated anti-αvβ5 integrin or (E) AlexaFluor-488 conjugated anti-α9β1 integrin antibodies for 1 hour at 4°C compared to cells incubated with an isotype-matched IgG-control. Samples were run on a Beckman-Coulter EPICS XL-MCL flow cytometer (N = 3).
(TIF)

S3 Fig. SUM-159 human breast cancer cells express CD44 and multiple different cell surface integrins. Representative histograms are shown from flow cytometry characterization of MDA-MB-231 cells incubated with (A) PE-conjugated anti-CD44, (B) AlexaFluor-488-conjugated anti-β1 integrin, (C) FITC-conjugated anti-αvβ3 integrin, (D) AlexaFluor-488-conjugated anti-αvβ5 integrin or (E) AlexaFluor-488 conjugated anti-α9β1 integrin antibodies for 1 hour at 4°C compared to cells incubated with an isotype-matched IgG-control. Samples were run on a Beckman-Coulter EPICS XL-MCL flow cytometer (N = 3).
(TIF)

S1 Table. Metastasis-associated proteins identified in bone marrow-conditioned media with the RayBio$^®$ Biotin label-based mouse antibody array.
(DOCX)

Acknowledgments

We thank Benjamin Hedley and Kristin Chadwick for their invaluable advice and technical help with the flow cytometry/FACS experiments, and Ann Chambers and Pieter Anbrough for helpful discussions during manuscript preparation.

Author Contributions

Conceptualization: GMP ALA.

Data curation: GMP MMP YX ALA.

Formal analysis: GMP MMP YX ALA.

Funding acquisition: ALA.

Investigation: GMP MMP YX ALA.

Methodology: GMP MMP YX JEC ALA.

Project administration: GMP YX ALA.

Resources: ALA.

Supervision: ALA.

Validation: GMP MMP JEC YX ALA.

Visualization: GMP ALA.

Writing – original draft: GMP MMP JEC YX ALA.

Writing – review & editing: GMP MMP JEC YX ALA.

References

1. Canadian Cancer Statistics Toronto, ON: Canadian Cancer Society; 2016 [updated 2016].

2. Miller KD, Siegel RL, Lin CC, Mariotto AB, Kramer JL, Rowland JH, et al. Cancer treatment and survivorship statistics, 2016. CA Cancer J Clin. 2016; 66(4):271–89. https://doi.org/10.3322/caac.21349 PMID: 27253694

3. Luzzi KJ, MacDonald IC, Schmidt EE, Kerkvliet N, Morris VL, Chambers AF, et al. Multistep nature of metastatic inefficiency: dormancy of solitary cells after successful extravasation and limited survival of early micrometastases. Am J Pathol. 1998; 153(3):865–73. https://doi.org/10.1016/S0002-9440(10)65628-3 PMID: 9736035

4. Charafe-Jauffret E, Ginestier C, Iovino F, Wicinski J, Cervera N, Finetti P, et al. Breast cancer cell lines contain functional cancer stem cells with metastatic capacity and a distinct molecular signature. Cancer Res. 2009; 69(4):1302–13. https://doi.org/10.1158/0008-5472.CAN-08-2741 PMID: 19190339

5. Visvader JE, Lindeman GJ. Cancer stem cells in solid tumours: accumulating evidence and unresolved questions. Nat Rev Cancer. 2008; 8(10):755–68. https://doi.org/10.1038/nrc2499 PMID: 18784658

6. Campbell LL, Polyak K. Breast tumor heterogeneity: cancer stem cells or clonal evolution? Cell Cycle. 2007; 6(19):2332–8. https://doi.org/10.4161/cc.6.19.4914 PMID: 17786053

7. Croker AK, Allan AL. Cancer stem cells: implications for the progression and treatment of metastatic disease. J Cell Mol Med. 2008; 12(2):374–90. https://doi.org/10.1111/j.1582-4934.2007.00211.x PMID: 18182063

8. Al-Hajj M, Wicha MS, Benito-Hernandez A, Morrison SJ, Clarke MF. Prospective identification of tumorigenic breast cancer cells. Proc Natl Acad Sci USA. 2003; 100(7):3983–8. https://doi.org/10.1073/pnas.0530291100 PMID: 12629218

9. Ginestier C, Hur MH, Charafe-Jauffret E, Monville F, Dutcher J, Brown M, et al. ALDH1 is a marker of normal and malignant human mammary stem cells and a predictor of poor clinical outcome. Cell Stem Cell. 2007; 1(5):555–67. https://doi.org/10.1016/j.stem.2007.08.014 PMID: 18371393

10. Croker AK, Goodale D, Chu J, Postenka C, Hedley BD, Hess DA, et al. High aldehyde dehydrogenase and expression of cancer stem cell markers selects for breast cancer cells with enhanced malignant and metastatic ability. J Cell Mol Med. 2009; 13(8B):2236–52. https://doi.org/10.1111/j.1582-4934.2008.00455.x PMID: 18681906

11. Hess KR, Varadhachary GR, Taylor SH, Wei W, Raber MN, Lenzi R, et al. Metastatic patterns in adenocarcinoma. Cancer. 2006; 106(7):1624–33. https://doi.org/10.1002/cncr.21778 PMID: 16518827

12. Weiss L. Comments on hematogenous metastatic patterns in humans as revealed by autopsy. Clin Exp Metastasis. 1992; 10(3):191–9. PMID: 1582089

13. Paget S. The distribution of secondary growths in cancer of the breast. 1889. Cancer Metastasis Rev. 1989; 8(2):98–101. PMID: 2673568

14. Coleman RE, Rubens RD. The clinical course of bone metastases from breast cancer. Br J Cancer. 1987; 55(1):61–6. PMID: 3814476

15. Pantel K, Brakenhoff RH. Dissecting the metastatic cascade. Nat Rev Cancer. 2004; 4(6):448–56. https://doi.org/10.1038/nrc1370 PMID: 15170447

16. Guise T. Examining the metastatic niche: targeting the microenvironment. Semin Oncol. 2010; 37 Suppl 2:S2–14.

17. Calvi LM, Link DC. The hematopoietic stem cell niche in homeostasis and disease. Blood. 2015; 126 (22):2443–51. https://doi.org/10.1182/blood-2015-07-533588 PMID: 26468230

18. Balic M, Lin H, Young L, Hawes D, Giuliano A, McNamara G, et al. Most early disseminated cancer cells detected in bone marrow of breast cancer patients have a putative breast cancer stem cell phenotype. Clin Cancer Res. 2006; 12(19):5615–21. https://doi.org/10.1158/1078-0432.CCR-06-0169 PMID: 17020963

19. Ling LJ, Wang S, Liu XA, Shen EC, Ding Q, Lu C, et al. A novel mouse model of human breast cancer stem-like cells with high CD44+CD24-/lower phenotype metastasis to human bone. Chin Med J (Engl). 2008; 121(20):1980–6.

20. Chu JE, Xia Y, Chin-Yee B, Goodale D, Croker AK, Allan AL. Lung-Derived Factors Mediate Breast Cancer Cell Migration through CD44 Receptor-Ligand Interactions in a Novel Ex Vivo System for Analysis of Organ-Specific Soluble Proteins. Neoplasia. 2014; 16(2):180–IN27. https://doi.org/10.1593/neo.132076 PMID: 24709425

21. Shevde LA, Das S, Clark DW, Samant RS. Osteopontin: an effector and an effect of tumor metastasis. Curr Mol Med. 2010; 10(1):71–81. PMID: 20205680

22. Furger KA, Allan AL, Wilson SM, Hota C, Vantyghem SA, Postenka CO, et al. Beta(3) integrin expression increases breast carcinoma cell responsiveness to the malignancy-enhancing effects of osteopontin. Mol Cancer Res. 2003; 1(11):810–9. PMID: 14517343

23. Allan AL, George R, Vantyghem SA, Lee MW, Hodgson NC, Engel CJ, et al. Role of the integrin-binding protein osteopontin in lymphatic metastasis of breast cancer. Am J Pathol. 2006; 169(1):233–46. https://doi.org/10.2353/ajpath.2006.051152 PMID: 16816376

24. Tuck AB, Chambers AF, Allan AL. Osteopontin overexpression in breast cancer: knowledge gained and possible implications for clinical management. J Cell Biochem. 2007; 102(4):859–68. https://doi.org/10.1002/jcb.21520 PMID: 17721886

25. Anborgh PH, Caria LB, Chambers AF, Tuck AB, Stitt LW, Brackstone M. Role of plasma osteopontin as a biomarker in locally advanced breast cancer. Am J Transl Res. 2015; 7(4):723–32. PMID: 26064440

26. Bramwell VH, Doig GS, Tuck AB, Wilson SM, Tonkin KS, Tomiak A, et al. Serial plasma osteopontin levels have prognostic value in metastatic breast cancer. Clin Cancer Res. 2006; 12(11 Pt 1):3337–43.

27. Singhal H, Bautista DS, Tonkin KS, O'Malley FP, Tuck AB, Chambers AF, et al. Elevated plasma osteopontin in metastatic breast cancer associated with increased tumor burden and decreased survival. Clin Cancer Res. 1997; 3(4):605–11. PMID: 9815727

28. Cailleau R, Olive M, Cruciger QV. Long-term human breast carcinoma cell lines of metastatic origin: preliminary characterization. In Vitro. 1978; 14(11):911–5. PMID: 730202

29. Forozan F, Veldman R, Ammerman CA, Parsa NZ, Kallioniemi A, Kallioniemi OP, et al. Molecular cytogenetic analysis of 11 new breast cancer cell lines. Br J Cancer. 1999; 81(8):1328–34. https://doi.org/10.1038/sj.bjc.6695007 PMID: 10604729

30. Xuan JW, Hota C, Chambers AF. Recombinant GST-human osteopontin fusion protein is functional in RGD-dependent cell adhesion. J Cell Biochem. 1994; 54(2):247–55. https://doi.org/10.1002/jcb.240540213 PMID: 8175899

31. Croker AK, Allan AL. Inhibition of aldehyde dehydrogenase (ALDH) activity reduces chemotherapy and radiation resistance of stem-like ALDHhiCD44(+) human breast cancer cells. Breast Cancer Res Treat. 2012; 133(1):75–87. https://doi.org/10.1007/s10549-011-1692-y PMID: 21818590

32. Ruoslahti E. RGD and other recognition sequences for integrins. Annu Rev Cell Dev Biol. 1996; 12:697–715. https://doi.org/10.1146/annurev.cellbio.12.1.697 PMID: 8970741

33. Andersen JN, Sathyanarayanan S, Di Bacco A, Chi A, Zhang T, Chen AH, et al. Pathway-based identification of biomarkers for targeted therapeutics: personalized oncology with PI3K pathway inhibitors. Sci Transl Med. 2010; 2(43):43ra55. https://doi.org/10.1126/scitranslmed.3001065 PMID: 20686178

34. Lipton A, Uzzo R, Amato RJ, Ellis GK, Hakimian B, Roodman GD, et al. The science and practice of bone health in oncology: managing bone loss and metastasis in patients with solid tumors. J Natl Compr Canc Netw. 2009; 7 Suppl 7:S1–29; quiz S30.

35. Sterling JA, Edwards JR, Martin TJ, Mundy GR. Advances in the biology of bone metastasis: how the skeleton affects tumor behavior. Bone. 2011; 48(1):6–15. https://doi.org/10.1016/j.bone.2010.07.015 PMID: 20643235

36. Gillespie MT, Thomas RJ, Pu ZY, Zhou H, Martin TJ, Findlay DM. Calcitonin receptors, bone sialoprotein and osteopontin are expressed in primary breast cancers. Int J Cancer. 1997; 73(6):812–5. PMID: 9399657

37. Ue T, Yokozaki H, Kitadai Y, Yamamoto S, Yasui W, Ishikawa T, et al. Co-expression of osteopontin and CD44v9 in gastric cancer. Int J Cancer. 1998; 79(2):127–32. PMID: 9583725

38. Kim JH, Skates SJ, Uede T, Wong KK, Schorge JO, Feltmate CM, et al. Osteopontin as a potential diagnostic biomarker for ovarian cancer. JAMA. 2002; 287(13):1671–9. PMID: 11926891

39. Standal T, Borset M, Sundan A. Role of osteopontin in adhesion, migration, cell survival and bone remodeling. Exp Oncol. 2004; 26(3):179–84. PMID: 15494684

40. Standal T, Hjorth-Hansen H, Rasmussen T, Dahl IM, Lenhoff S, Brenne AT, et al. Osteopontin is an adhesive factor for myeloma cells and is found in increased levels in plasma from patients with multiple myeloma. Haematologica. 2004; 89(2):174–82. PMID: 15003892

41. Tuck AB, Chambers AF. The role of osteopontin in breast cancer: clinical and experimental studies. J Mammary Gland Biol Neoplasia. 2001; 6(4):419–29. PMID: 12013531

42. Tuck AB, Elliott BE, Hota C, Tremblay E, Chambers AF. Osteopontin-induced, integrin-dependent migration of human mammary epithelial cells involves activation of the hepatocyte growth factor receptor (Met). J Cell Biochem. 2000; 78(3):465–75. PMID: 10861844

43. Tuck AB, Hota C, Chambers AF. Osteopontin(OPN)-induced increase in human mammary epithelial cell invasiveness is urokinase (uPA)-dependent. Breast Cancer Res Treat. 2001; 70(3):197–204. PMID: 11804183

44. Tuck AB, Hota C, Wilson SM, Chambers AF. Osteopontin-induced migration of human mammary epithelial cells involves activation of EGF receptor and multiple signal transduction pathways. Oncogene. 2003; 22(8):1198–205. https://doi.org/10.1038/sj.onc.1206209 PMID: 12606946

45. Tuck AB, O'Malley FP, Singhal H, Harris JF, Tonkin KS, Kerkvliet N, et al. Osteopontin expression in a group of lymph node negative breast cancer patients. Int J Cancer. 1998; 79(5):502–8. PMID: 9761120

46. Khan SA, Cook AC, Kappil M, Gunthert U, Chambers AF, Tuck AB, et al. Enhanced cell surface CD44 variant (v6, v9) expression by osteopontin in breast cancer epithelial cells facilitates tumor cell migration: novel post-transcriptional, post-translational regulation. Clin Exp Metastasis. 2005; 22(8):663–73. https://doi.org/10.1007/s10585-006-9007-0 PMID: 16691370

47. Nemoto H, Rittling SR, Yoshitake H, Furuya K, Amagasa T, Tsuji K, et al. Osteopontin deficiency reduces experimental tumor cell metastasis to bone and soft tissues. J Bone Miner Res. 2001; 16 (4):652–9. https://doi.org/10.1359/jbmr.2001.16.4.652 PMID: 11315992

48. Rota LM, Lazzarino DA, Ziegler AN, LeRoith D, Wood TL. Determining mammosphere-forming potential: application of the limiting dilution analysis. J Mammary Gland Biol Neoplasia. 2012; 17(2):119–23. https://doi.org/10.1007/s10911-012-9258-0 PMID: 22678420

49. Haylock DN, Nilsson SK. Stem cell regulation by the hematopoietic stem cell niche. Cell Cycle. 2005; 4 (10):1353–5. https://doi.org/10.4161/cc.4.10.2056 PMID: 16123595

50. Levesque JP, Helwani FM, Winkler IG. The endosteal 'osteoblastic' niche and its role in hematopoietic stem cell homing and mobilization. Leukemia. 2010; 24(12):1979–92. https://doi.org/10.1038/leu.2010.214 PMID: 20861913

51. Taichman RS, Reilly MJ, Emerson SG. Human osteoblasts support human hematopoietic progenitor cells in vitro bone marrow cultures. Blood. 1996; 87(2):518–24. PMID: 8555473

52. Nilsson SK, Johnston HM, Whitty GA, Williams B, Webb RJ, Denhardt DT, et al. Osteopontin, a key component of the hematopoietic stem cell niche and regulator of primitive hematopoietic progenitor cells. Blood. 2005; 106(4):1232–9. https://doi.org/10.1182/blood-2004-11-4422 PMID: 15845900

53. Olechnowicz SW, Edwards CM. Contributions of the host microenvironment to cancer-induced bone disease. Cancer Res. 2014; 74(6):1625–31. https://doi.org/10.1158/0008-5472.CAN-13-2645 PMID: 24599133

54. Pietras A, Katz AM, Ekstrom EJ, Wee B, Halliday JJ, Pitter KL, et al. Osteopontin-CD44 signaling in the glioma perivascular niche enhances cancer stem cell phenotypes and promotes aggressive tumor growth. Cell Stem Cell. 2014; 14(3):357–69. https://doi.org/10.1016/j.stem.2014.01.005 PMID: 24607407

55. Louderbough JM, Schroeder JA. Understanding the dual nature of CD44 in breast cancer progression. Mol Cancer Res. 2011; 9(12):1573–86. https://doi.org/10.1158/1541-7786.MCR-11-0156 PMID: 21970856

56. Benoit YD, Groulx JF, Gagne D, Beaulieu JF. RGD-Dependent Epithelial Cell-Matrix Interactions in the Human Intestinal Crypt. J Signal Transduct. 2012; 2012:248759. https://doi.org/10.1155/2012/248759 PMID: 22988499

57. Sun X, Gao L, Yu RK, Zeng G. Down-regulation of WNK1 protein kinase in neural progenitor cells suppresses cell proliferation and migration. J Neurochem. 2006; 99(4):1114–21. https://doi.org/10.1111/j.1471-4159.2006.04159.x PMID: 17018027

58. Moniz S, Jordan P. Emerging roles for WNK kinases in cancer. Cell Mol Life Sci. 2010; 67(8):1265–76. https://doi.org/10.1007/s00018-010-0261-6 PMID: 20094755

59. Lee BH, Chen W, Stippec S, Cobb MH. Biological cross-talk between WNK1 and the transforming growth factor beta-Smad signaling pathway. J Biol Chem. 2007; 282(25):17985–96. https://doi.org/10.1074/jbc.M702664200 PMID: 17392271

60. Zhang Z, Xu X, Zhang Y, Zhou J, Yu Z, He C. LINGO-1 interacts with WNK1 to regulate nogo-induced inhibition of neurite extension. J Biol Chem. 2009; 284(23):15717–28. https://doi.org/10.1074/jbc.M808751200 PMID: 19363035

61. Ridley AJ, Schwartz MA, Burridge K, Firtel RA, Ginsberg MH, Borisy G, et al. Cell migration: integrating signals from front to back. Science. 2003; 302(5651):1704–9. https://doi.org/10.1126/science.1092053 PMID: 14657486

62. Zhang H, Guo M, Chen JH, Wang Z, Du XF, Liu PX, et al. Osteopontin knockdown inhibits alphav,beta3 integrin-induced cell migration and invasion and promotes apoptosis of breast cancer cells by inducing autophagy and inactivating the PI3K/Akt/mTOR pathway. Cell Physiol Biochem. 2014; 33(4):991–1002. https://doi.org/10.1159/000358670 PMID: 24714122

63. Nanni P, Nicoletti G, Palladini A, Croci S, Murgo A, Ianzano ML, et al. Multiorgan metastasis of human HER-2+ breast cancer in Rag2-/-;Il2rg-/- mice and treatment with PI3K inhibitor. PLoS One. 2012; 7(6):e39626. https://doi.org/10.1371/journal.pone.0039626 PMID: 22737248

64. Wander SA, Zhao D, Besser AH, Hong F, Wei J, Ince TA, et al. PI3K/mTOR inhibition can impair tumor invasion and metastasis in vivo despite a lack of antiproliferative action in vitro: implications for targeted therapy. Breast Cancer Res Treat. 2013; 138(2):369–81. https://doi.org/10.1007/s10549-012-2389-6 PMID: 23430223